

Detection of dissolved metals using a liquid electrode dielectric barrier discharge

T. Krähling¹, S. Müller¹, S. Groh², J. Franzke¹

¹ISAS – Leibniz-Institut für Analytische Wissenschaften, Otto-Hahn-Str. 6b, 44227 Dortmund, Germany

²ISAS – Leibniz-Institut für Analytische Wissenschaften, Bunsen-Kirchhoff-Str. 11, 44139 Dortmund, Germany

Analysis of dissolved metals in liquid samples using a dielectric barrier discharge with flowing liquid electrode has been studied. Inside a fused-silica capillary the discharge is ignited between the liquid surface and a tungsten electrode, driven by a pulsed high voltage. In this manner the flowing liquid acts as second electrode itself and the wall of the capillary as dielectric barrier. Due to a pulsation of the electrode gap the discharge is sustainable for one hour and more. Calibration measurements are performed for several alkali, alkaline earth metals and silver. With a flow rate of $20 \mu\text{L min}^{-1}$ detection limits between 0.02 mg L^{-1} for potassium and 6.9 mg L^{-1} for barium are determined. Application as metal detection system for environmental liquid samples as well as monitoring device in flow systems seems possible.

1. Introduction

Using miniaturized systems is a recent trend in analytical spectrometry. Scaling down the dimensions of all components, from sampling, sample preparation, separation techniques up to detection systems, are studied by scientists in various fields to build small analytical devices with small sample consumption, less analysis time and reduced cost. In analytical chemistry miniaturized discharges are used, among others, as soft ionization source for mass spectrometry and ion mobility spectroscopy or as excitation source for optical emission spectrometry. A recent overview is given by Meyer et al. [1, 2].

Tombrink et al. [3] introduced an arrangement for liquid analysis, where the discharge is ignited inside a fused-silica capillary between a flowing liquid and a metal electrode. A very low flow rate of just $\mu\text{L min}^{-1}$, low power consumption and the operation at atmospheric pressure without additional gases are advantages of this system. Dissolved metals in the liquid electrode are detected by optical emission spectrometry (OES) and the limits of detection (LOD) for Sr, Pb and Hg are reported with 18, 40, and 42 mg L^{-1} .

In the presented study, we use a slightly enlarged arrangement called liquid electrode dielectric barrier discharge (LE-DBD). With the performed modifications the discharge be operated with higher flow rates and improved long-time stability is achieved. Detection limits

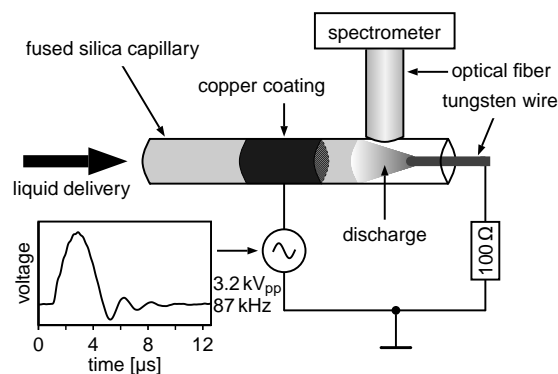


Fig. 1: Experimental arrangement of the LE-DBD

for several alkali, alkaline earth metals and silver are determined to compare the analytical performance with other systems.

2. Experimental arrangement

The experimental arrangement of the LE-DBD is shown in Fig. 1. A syringe pump system is connected to a 100 mm long polyimide-covered fused-silica capillary (i.d. $700 \mu\text{m}$, o.d. $850 \mu\text{m}$) with silicone tube and ensure a constant delivery rate of the liquid solution (1 mol L^{-1} nitric acid, $20 \mu\text{L min}^{-1}$ flow rate). At the other side of the capillary a tungsten wire ($\varnothing 400 \mu\text{m}$) is inserted and stays open to ambient air. The tungsten wire with an insertion length of around $900 \mu\text{m}$ acts as counter electrode and is connected to ground over a 100Ω current limiting resistor. A 200 nm cop-

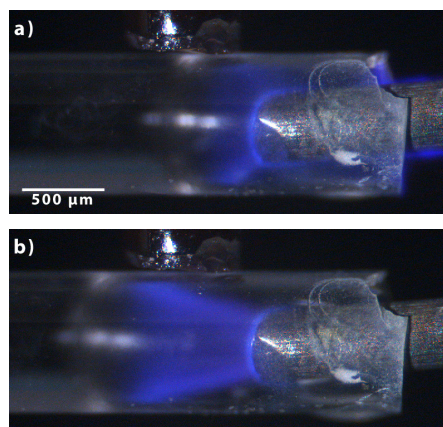


Fig. 2: Pulsation of the LE-DBD discharge. Picture a) shows the discharge after ignition where the trapezoid shape is not completely established and b) the plasma shortly before reaching its maximum size.

per layer with a length of 24 mm is sputtered on the outer surface of the capillary, where the layer begins 11 mm away from the open end, and is connected to a home-made high voltage peak generator in the kHz range. In this arrangement the copper layer acts as ring electrode and the capillary wall as dielectric barrier. The applied high voltage (3.2 kV_{pp}, 87 kHz) is capacitively coupled into the liquid and a plasma is formed between liquid meniscus and tungsten electrode.

For adjustment and direct observation of the discharge a CCD microscope camera (Leica DFC420 C) is used (not shown in fig. 1). The emitted light from the plasma is collected by an optical fiber (\varnothing 600 μ m), adjusted perpendicular to the capillary, and is connected to a portable spectrometer (OceanOptics USB4000, 200 – 900 nm). Analysed metals are the alkalis Li, K, Rb, and Cs, the alkaline earths Mg, Ca, Sr, and Ba and the transition metal Ag. Stock solutions for the liquid electrode containing the analyte are prepared from deionized water, nitric acid and metal salts.

3. Results and discussion

Other than by Tombrink et al. [3] the discharge shows an pulsation of the electrode gap (fig. 2). The discharge ignites independently once the distance between liquid meniscus and tungsten electrode is about 200 μ m. Shortly after ignition, the plasma fills almost the entire space between the liquid meniscus and tungsten electrode. Due to the different diameters of the both electrodes the plasma shows a typical trapezoid shape. While

the discharge is ignited, more liquid is removed from the liquid boundary layer and transferred into the discharge as the constant flow rate delivers. This increases the gap between liquid meniscus and tungsten electrode, which also increases the plasma volume. At an electrode gap of around 900 μ m the plasma reaches its maximum size and extinguishes. The gap decreases through the flow rate of the liquid as long as the next ignition starts. The length of a cycle is approximately 1.7 s, where the plasma burning time is in the range of 0.5 s. Thereby the pulsation frequency is not influenced by solved analyte over several magnitudes of concentration. Gas bubbles, that arise during the burning time, are collected through the pulsation of the liquid meniscus and do not extinguish the discharge. Therefore, this pulsation is the main influence factor for long-time stability and the discharge can be established for one hour and more.

Fig. 3 shows a characteristic emission spectrum of dissolved strontium nitrate in 1 mol L⁻¹ nitric acid and the intensity is normalised to the maximum scale of the spectrometer. Emission lines and bands, which are always observed by using nitric acid in aqueous solution, are molecular emissions from OH and NO radical around 300 nm, as well as atomic emissions from hydrogen (H $_{\alpha}$, H $_{\beta}$) and oxygen (triplets at 777 nm and 844 nm). Even though operation under ambient air emission of molecular nitrogen is not observed. Emissions from strontium are the lines at 460.7 nm (Sr I, transition 5s² ¹S₀ \leftarrow 5s5p ¹P₁^o), 407.8 nm and 421.6 nm (Sr II, transitions 5s ²S_{1/2} \leftarrow 5p ²P_{3/2}^o

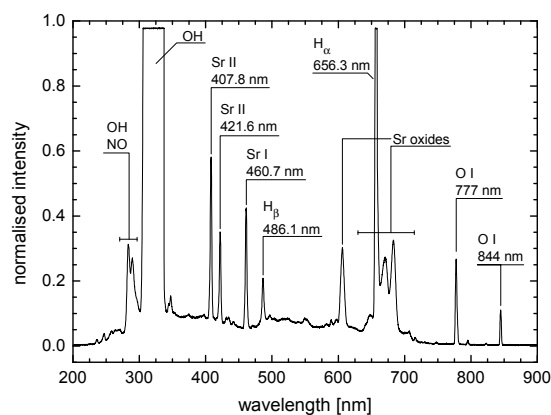


Fig. 3: Characteristic emission spectrum of 438 mg L⁻¹ Sr in 1 mol L⁻¹ nitric acid, measured with 100 ms integration time.

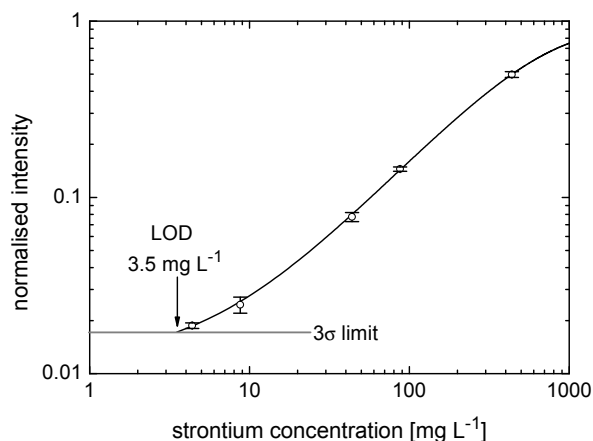


Fig. 4: Calibration curve for Sr in 1 mol L⁻¹ nitric acid using the 407,8 nm Sr II emission line.

and $5s^2S_{1/2} \leftarrow 5p^2P_{1/2}^o$), respectively. The molecular bands around 605 nm as well as around 670 nm are caused by strontium oxides, where this oxides can be SrO, SrOH, as well as SrO₂ and Sr(OH)₂ [4].

For all measured alkaline earth metals emissions from neutral and single ionized atoms are observed, whereas Mg shows no emission from oxides. Alkali metals and Ag show only emissions from neutral atoms. The occurrence of alkaline earth oxides are well known in the field of graphite furnace atomic absorption spectroscopy and indicates a thermal evaporation, whereas the appearance of single ionized alkaline earth can be explained by a transfer of matter from the liquid boundary layer into the plasma by a form of electrospray. From this, we assume that the liquid transfer into the plasma is a process with at least two mechanisms. This should be investigated in further studies.

Due to the pulsation of the discharge for the calibration measurements we acquire spectra continuously for 45 s with an integration time of 100 ms, determine the maximum intensity per cycle for a certain emission line and average them after eliminating outliers using a Hampel test [5]. Fig. 4 shows the calibration curve for strontium using the 406.8 nm Sr II emission line. The calibration curve shows an exponential decay shape and is observable for all investigated metals as well as for the strontium oxides. The reached LODs are for the alkali metals Li, K, Rb, and Cs 0.028, 0.020, 0.60, and 1.3 mg L⁻¹, respectively. For the alkaline earth metals the LODs are one to two orders of magnitude higher and are determined

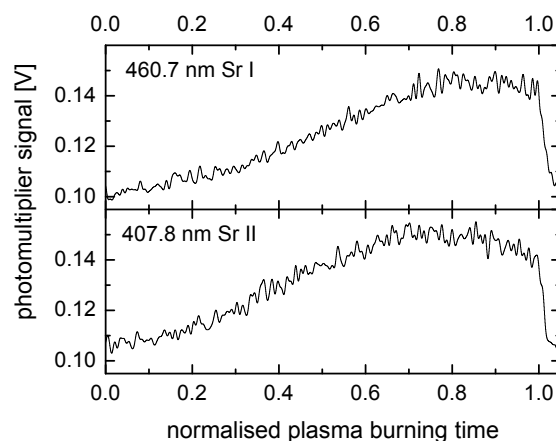


Fig. 5: Time development of the both strongest Sr emission lines during a plasma burning time.

for Mg, Ca, Sr, and Ba with 1.7, 1.2, 3.5, and 6.9 mg L⁻¹, respectively. Even though the integration time for Ag is reduced to 25 ms the LOD is determined with 0.54 mg L⁻¹. A commercial available device is the MH-5000 for liquid analysis (Micro Emission, Japan) and uses the liquid electrode plasma optical emission spectrometry (LEP-OES) [6, 7] technique. Comparing the LE-DBD with the MH-5000 shows, that the LODs reached with the LE-DBD are up to two orders of magnitude lower. Only for Ag and Mg the LODs are in the same range.

Noticeable is, that for the alkaline earth metals the intensity of the strongest single ionized emission line is equal or slightly higher than that emission from the strongest neutral atomic line. Therefore, the determination of the LOD using the emission line of single ionized atoms are the better choice. In fig. 5 the time development of two emission lines from Sr during a plasma burning time are shown. For these measurements a McPearson EU700 spectrometer with 100 μm slit width and 1200 lines per mm grating together with an Electron Tubes 9202B photomultiplier is used. Due to the spreading of plasma burning time and in order to make a comparison of the time development of the emission lines possible the time axis is normalized to the plasma burning time. It is obvious, that the intensity increases during the plasma burning time, where a main component for this behaviour is the increasing plasma volume during the burning time. Both the Sr I and the Sr II line reaches the intensity maximum during the burning time and nearly hold it for about 150 ms (0.3 normalized plasma

burning time). But the time, when the maximum is reached, is different for the both emission lines. While for the Sr I line the intensity maximum is reached in the last part of the burning time, the maximum for the Sr II occurs earlier and already before the plasma extinguishes the intensity decreases again. From this behaviour it is clear, why for the determination of the LOD the Sr II line is preferred and shows also, that a higher integration time can not result in lower detection limits with a low spreading of the measured intensity signals over several discharge cycles.

4. Conclusion

The liquid electrode dielectric barrier discharge (LE-DBD) was applied for the detection of several metals dissolved in the flowing liquid electrode with a flow rate of only $20 \mu\text{L min}^{-1}$. The slightly enlargement of the system compared to the previously reported system results in a pulsation of the discharge, where the discharge cycle between a plasma burning phase with increasing electrode gap and a plasma extinguishing phase with decreasing electrode gap. This pulsation influences the long-term stability of the discharge positively. Furthermore the LE-DBD shows a good detection limit for the studied alkali, alkaline earth metals and silver, where the achieved LODs are between 0.02 mg L^{-1} for K and 6.9 mg L^{-1} for Ba at low sample volumes. Application as metal detection system for environmental liquid samples as well as monitoring device in flow systems seems to be possible.

5. Acknowledgments

The financial support by the Ministerium für Innovation, Wissenschaft, Forschung und Technologie des Landes Nordrhein-Westfalen, by the Bundesministerium für Bildung und Forschung and by the Deutsche Forschungsgemeinschaft is gratefully acknowledged.

6. References

- [1] C. Meyer, S. Müller, E.L. Gurevich, J. Franzke, *Analyst* (2010), doi:10.1039/C0AN00994F
- [2] C. Meyer, S. Müller, T. Krähling, A. Michels, J. Franzke, in *Encyclopedia of Analytical Chemistry*, ed. R. A. Meyers, John Wiley & Sons Ltd, in press.
- [3] S. Tombrink, S. Müller, R. Heming, A. Michels, P. Lampen, J. Franzke, *Anal. Bioanal. Chem.* 397 (2010) 2917.
- [4] L.J. Prell, D.L. Styrus, D.A. Redfield, *J. Anal. Atom. Spectrom.* 6 (1991) 25.
- [5] J.-M. Mermet, in *Encyclopedia of Analytical Chemistry*, ed. R. A. Meyers, John Wiley & Sons Ltd, 2009.
- [6] C.G. Wilson, Y.B. Gianchandani, *IEEE T. Electron. Dev.* 49 (2002) 2317.
- [7] H. Matsumoto, A. Iiduka, T. Yamamoto, E. Tamiya, Y. Takamura, in 9th International conference on Miniaturized Systems for Chemistry and Life Sciences, Boston, 2005.